

# Seismic vulnerability, behavior and design of tunnel form building structures

Can Balkaya<sup>a</sup>, Erol Kalkan<sup>b,\*</sup>

<sup>a</sup> Department of Civil Engineering, Middle East Technical University, Ankara 06531, Turkey

<sup>b</sup> Department of Civil and Environmental Engineering, University of California Davis, Davis, CA 95616, USA

Received 28 March 2003; received in revised form 3 July 2004; accepted 14 July 2004

## Abstract

Multi-story reinforced concrete tunnel form buildings are one of the common structural types in regions prone to high seismic risk due to the buildings inherent earthquake resistance and ease of construction. Despite their good performance during earthquakes in 1999 in Turkey, and abundance of such structures scattered worldwide, current seismic codes and design provisions provide insufficient guidelines for their seismic design. As a compensatory measure, a series of modal and nonlinear static analyses are conducted by emphasizing the characteristic dynamic behavior of tunnel form buildings including impacts of wall-to-wall and wall-to-slab interaction and effects of torsion and wall-openings on the load transfer mechanism and seismic performance. A new formula for explicit determination of their fundamental period is developed in addition to a recommended response reduction factor and reinforcement detailing around shear-wall openings.

© 2004 Elsevier Ltd. All rights reserved.

*Keywords:* Tunnel form building; Inelasticity; Shear-wall; Pushover analysis; Response modification factor; Fundamental period; Reinforcement

## 1. Introduction

Multi-story reinforced concrete (RC) tunnel form buildings (i.e., box type buildings) are been increasingly constructed worldwide. The main components of a tunnel form system are its relatively thinner shear-walls and flat-slabs compared to those of traditional RC buildings. Shear-walls in tunnel form buildings are utilized as the primary lateral load resisting and vertical load carrying members due to the absence of beams and columns. Typical implementation of the tunnel form system and its details are exhibited in Fig. 1. In a tunnel form system, load carrying pre-cast members are avoided, whereas nonstructural pre-cast elements such as RC stairs and outside facade panels are commonly used to expedite construction. Continuity of shear-walls throughout the height is recommended to avoid local stress concentrations and to minimize

torsion. Such a strict shear-wall configuration in the plan and throughout the height of the building may limit the interior space use from an architectural point of view, and this is one of the disadvantages of tunnel form buildings. During construction, walls and slabs, having almost the same thickness, are cast in a single operation. This process reduces not only the number of cold-formed joints, but also the assembly time. The simultaneous casting of walls and slabs results in monolithic structures unlike any other frame-type RC buildings. Consequently, tunnel form buildings gain enhanced seismic performance by retarding plastic hinge formations at the most critical locations, such as slab-wall connections and around wall openings.

Seismic performances of tunnel form buildings have been observed during earthquakes ( $M_W$  7.4 Kocaeli and  $M_W$  7.2 Duzce) in Turkey in 1999. These earthquakes struck the most populated areas, and caused substantial structural damage, casualties and economic loss. However, in the aftermath of these events, neither demolished nor damaged tunnel form buildings located in the vicinity of the worst-hit regions were reported in

\* Corresponding author. Tel.: +1-530-754-4958; fax: +1-530-752-7872.

E-mail address: [ekalkan@ucdavis.edu](mailto:ekalkan@ucdavis.edu) (E. Kalkan).

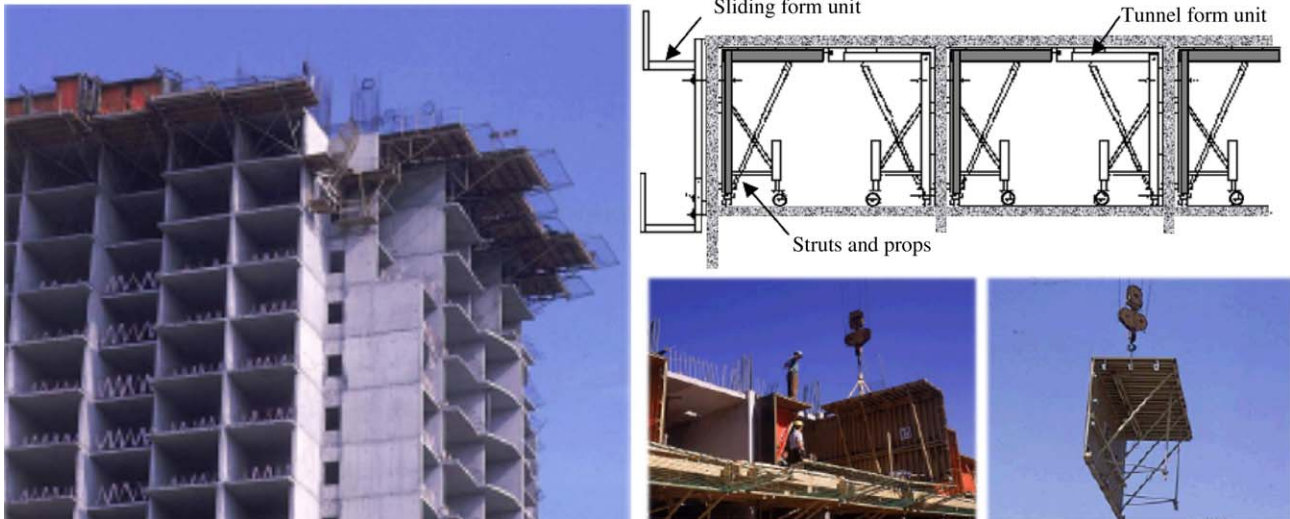


Fig. 1. Tunnel form construction technique and its special formwork system.

contrast to the severely damaged conditions of many conventional RC buildings. Such a creditable performance of tunnel form buildings has aided their construction in Turkey as a replacement of many severely damaged and collapsed RC buildings. Not only in Turkey, but also in many other countries prone to seismic risk, tunnel form buildings are gaining increasing popularity. This accentuates an urgent need to clarify seismic behavior, design and safety issues of these buildings.

In this study, consistency of code-based empirical formulas to estimate the fundamental period of buildings was evaluated for tunnel form buildings. The comparative analysis results reveal that common formulas involving the Turkish Seismic Code, TSC [27] and the Uniform Building Code [23] may yield inaccurate results for explicit determination of their fundamental period. Based on the premise that such formulas are commonly used in engineering practice, a new predictive equation is proposed in this paper. This equation was developed based on the finite element analysis of 140 buildings having a variety of plans, heights and wall-configurations. This equation and the values of its estimating parameters are introduced in the first part of the paper. The seismic performance evaluation is next presented based on the inelastic static analyses of two representative case studies. To accomplish detailed three-dimensional (3D) analyses on shear-wall dominant systems, a nonlinear isoparametric shell element having opening-closing and rotating crack capabilities was utilized. Thus, the seismic behavior of tunnel form buildings was investigated more efficiently without necessitating any simplifications in the finite element models (e.g., use of a rigid beam as a link element and/or a wide beam-column element for shear-wall modeling). This efficiency further facilitated the investigation

of the 3D behavior, diaphragm flexibility, slab-wall interaction and torsion. The stress concentration and shear flow around the shear-wall openings and their reinforcement detailing were also studied. The results obtained from the 3D models were compared with those of the 2D models. In the final part, the value of a consistent response modification factor ( $R$ -factor) is introduced for a typical tunnel form building.

## 2. A simple formula development for fundamental period estimation

It is a customary practice to obtain the lower bound fundamental period of a structure via code-given expressions to establish the proper design force level unless modal analysis based on the detailed finite element model is conducted. Therefore, accurate estimation of the fundamental period is inevitably essential to calculate the reliable design forces. It has long been recognized that significant errors tend to occur when the code-given equations such as those given in the UBC and the TSC are utilized for shear-wall dominant systems [11,25]. To compensate for this deficiency, Lee et al. [25] proposed a simple formula based on their experimental data to estimate the lower bound fundamental period of tunnel form buildings having stories  $\geq 15$ . A set of new formulas to estimate the period of such buildings having stories  $\leq 15$  has been recently developed by Balkaya and Kalkan [11]. The objective here is to present updated information on the period of tunnel form buildings using an extended building inventory as a continuation of our earlier work. In this paper, a simpler formula that can be applicable for both mid-rise (story level  $\leq 15$ ) and high-rise (story level  $> 15$ ) tunnel form buildings is developed

Table 1  
Structural and dynamic properties of tunnel form buildings

Plan No.	No. of story	Height (m)	Dimension (m)		Shear-wall area (m <sup>2</sup> )		FEM results		Predicted period, $T$ (s)		
			Length	Width	Length	Width	$T$ (s)	First mode	Eq. (1)	TSC98	UBC97
1	5	14.0	29.70	15.70	4.78	17.80	0.13	Long.	0.27	0.17	0.17
	10	28.0	29.70	15.70	4.78	17.80	0.29		0.53	0.38	0.37
	12	33.6	29.70	15.70	4.78	17.80	0.37		0.64	0.45	0.44
	15	42.0	29.70	15.70	4.78	17.80	0.49		0.80	0.55	0.54
	18	50.4	29.70	15.70	5.98	22.25	0.70		1.05	0.57	0.57
	20	56.0	29.70	15.70	7.97	29.67	0.74		1.31	0.54	0.54
	25	70.0	29.70	15.70	7.97	29.67	1.03		1.64	0.65	0.64
2	5	14.0	31.04	19.92	3.40	19.92	0.12	Long.	0.20	0.15	0.15
	10	28.0	31.04	19.92	3.40	19.92	0.28		0.40	0.35	0.35
	12	33.6	31.04	19.92	3.40	19.92	0.35		0.48	0.42	0.42
	15	42.0	31.04	19.92	3.40	19.92	0.47		0.60	0.52	0.52
	18	50.4	31.04	19.92	4.25	24.90	0.58		0.79	0.55	0.54
	20	56.0	31.04	19.92	5.67	33.20	0.64		0.99	0.52	0.52
	25	70.0	31.04	19.92	5.67	33.20	0.95		1.24	0.63	0.62
3	5	14.0	38.80	17.03	3.98	19.60	0.14	Long.	0.25	0.18	0.18
	10	28.0	38.80	17.03	3.98	19.60	0.31		0.49	0.39	0.39
	12	33.6	38.80	17.03	3.98	19.60	0.39		0.59	0.47	0.46
	15	42.0	38.80	17.03	3.98	19.60	0.50		0.74	0.57	0.57
	18	50.4	38.80	17.03	4.98	24.50	0.59		0.97	0.60	0.59
	20	56.0	38.80	17.03	6.64	32.67	0.64		1.21	0.57	0.56
	25	70.0	38.80	17.03	6.64	32.67	0.93		1.51	0.68	0.67
4	5	14.0	12.00	8.00	1.44	2.88	0.14	Trans.	0.25	0.32	0.32
	10	28.0	12.00	8.00	1.44	2.88	0.35		0.50	0.61	0.77
	12	33.6	12.00	8.00	1.44	2.88	0.49		0.60	0.70	0.94
	15	42.0	12.00	8.00	1.44	2.88	0.76		0.75	0.82	1.18
	18	50.4	12.00	8.00	1.80	3.60	1.01		0.99	0.95	1.25
	20	56.0	12.00	8.00	2.40	4.80	1.17		1.23	1.02	1.18
	25	70.0	12.00	8.00	2.40	4.80	1.81		1.54	1.21	1.43
5	5	14.0	12.00	8.00	3.84	1.92	0.16	Torsion	0.28	0.36	0.42
	10	28.0	12.00	8.00	3.84	1.92	0.43		0.56	0.61	0.80
	12	33.6	12.00	8.00	3.84	1.92	0.55		0.68	0.70	0.93
	15	42.0	12.00	8.00	3.84	1.92	0.74		0.84	0.82	1.12
	18	50.4	12.00	8.00	4.80	2.40	0.89		1.11	0.95	1.15
	20	56.0	12.00	8.00	6.40	3.20	0.97		1.38	1.02	1.08
	25	70.0	12.00	8.00	6.40	3.20	1.28		1.73	1.21	1.29
6	5	14.0	12.00	8.00	1.44	3.84	0.11	Long.	0.26	0.30	0.29
	10	28.0	12.00	8.00	1.44	3.84	0.32		0.53	0.61	0.71
	12	33.6	12.00	8.00	1.44	3.84	0.45		0.63	0.70	0.86
	15	42.0	12.00	8.00	1.44	3.84	0.69		0.79	0.82	1.07
	18	50.4	12.00	8.00	1.80	4.80	0.93		1.04	0.95	1.13
	20	56.0	12.00	8.00	2.40	6.40	1.08		1.29	1.02	1.08
	25	70.0	12.00	8.00	2.40	6.40	1.68		1.61	1.21	1.30
7	5	14.0	12.00	8.00	2.88	2.64	0.13	Torsion	0.29	0.36	0.46
	10	28.0	12.00	8.00	2.88	2.64	0.35		0.57	0.61	0.84
	12	33.6	12.00	8.00	2.88	2.64	0.50		0.69	0.70	0.97
	15	42.0	12.00	8.00	2.88	2.64	0.75		0.86	0.82	1.15
	18	50.4	12.00	8.00	3.60	3.30	1.02		1.13	0.95	1.19
	20	56.0	12.00	8.00	4.80	4.40	1.18		1.40	1.02	1.11
	25	70.0	12.00	8.00	4.80	4.40	1.83		1.75	1.21	1.32
8	5	14.0	38.80	17.03	3.98	19.60	0.14	Torsion	0.25	0.36	0.44
	10	28.0	38.80	17.03	3.98	19.60	0.44		0.49	0.61	0.81
	12	33.6	38.80	17.03	3.98	19.60	0.58		0.59	0.70	0.94
	15	42.0	38.80	17.03	3.98	19.60	0.82		0.74	0.82	1.12

(continued on next page)

Table 1 (continued)

Plan No.	No. of story	Height (m)	Dimension (m)		Shear-wall area (m <sup>2</sup> )		FEM results		Predicted period, $T$ (s)		
			Length	Width	Length	Width	$T$ (s)	First mode	Eq. (1)	TSC98	UBC97
	18	50.4	38.80	17.03	4.98	24.50	1.03		0.97	0.95	1.16
	20	56.0	38.80	17.03	6.64	32.67	1.15		1.21	1.02	1.09
	25	70.0	38.80	17.03	6.64	32.67	1.69		1.51	1.21	1.29
9	5	14.0	12.00	8.00	4.80	1.92	0.16	Torsion	0.29	0.36	0.40
	10	28.0	12.00	8.00	4.80	1.92	0.43		0.58	0.61	0.75
	12	33.6	12.00	8.00	4.80	1.92	0.55		0.70	0.70	0.87
	15	42.0	12.00	8.00	4.80	1.92	0.74		0.88	0.82	1.04
	18	50.4	12.00	8.00	6.00	2.40	0.89		1.15	0.95	1.07
	20	56.0	12.00	8.00	8.00	3.20	0.98		1.43	1.01	1.01
	25	70.0	12.00	8.00	8.00	3.20	1.28		1.79	1.20	1.19
10	5	14.0	35.00	20.00	7.20	12.96	0.16	Long.	0.23	0.17	0.17
	10	28.0	35.00	20.00	7.20	12.96	0.38		0.46	0.39	0.39
	12	33.6	35.00	20.00	7.20	12.96	0.48		0.55	0.47	0.46
	15	42.0	35.00	20.00	7.20	12.96	0.64		0.69	0.57	0.57
	18	50.4	35.00	20.00	9.00	16.20	0.80		0.90	0.60	0.59
	20	56.0	35.00	20.00	12.00	21.60	0.92		1.12	0.57	0.56
	25	70.0	35.00	20.00	12.00	21.60	1.22		1.40	0.68	0.67
11	5	14.0	11.00	9.00	2.64	1.80	0.23	Torsion	0.23	0.34	0.33
	10	28.0	11.00	9.00	2.64	1.80	0.63		0.46	0.61	0.79
	12	33.6	11.00	9.00	2.64	1.80	0.82		0.56	0.70	0.95
	15	42.0	11.00	9.00	2.64	1.80	0.83		0.69	0.82	1.18
	18	50.4	11.00	9.00	3.30	2.25	1.35		0.91	0.95	1.24
	20	56.0	11.00	9.00	4.40	3.00	1.44		1.14	1.02	1.18
	25	70.0	11.00	9.00	4.40	3.00	1.94		1.42	1.21	1.42
12	5	14.0	31.50	27.15	9.70	13.86	0.16	Torsion	0.19	0.26	0.26
	10	28.0	31.50	27.15	9.70	13.86	0.42		0.37	0.61	0.63
	12	33.6	31.50	27.15	9.70	13.86	0.55		0.45	0.70	0.76
	15	42.0	31.50	27.15	9.70	13.86	0.77		0.56	0.82	0.95
	18	50.4	31.50	27.15	12.13	17.33	0.98		0.73	0.95	1.00
	20	56.0	31.50	27.15	16.17	23.10	1.10		0.91	0.96	0.95
	25	70.0	31.50	27.15	16.17	23.10	1.54		1.14	1.16	1.15
13	5	14.0	25.50	25.04	10.70	10.88	0.14	Torsion	0.19	0.19	0.19
	10	28.0	25.50	25.04	10.70	10.88	0.40		0.38	0.41	0.41
	12	33.6	25.50	25.04	10.70	10.88	0.55		0.46	0.49	0.48
	15	42.0	25.50	25.04	10.70	10.88	0.80		0.57	0.59	0.59
	18	50.4	25.50	25.04	13.38	13.60	1.03		0.75	0.62	0.61
	20	56.0	25.50	25.04	17.83	18.13	1.17		0.94	0.59	0.58
	25	70.0	25.50	25.04	17.83	18.13	1.69		1.17	0.70	0.69
14	5	14.0	28.00	12.00	2.88	3.60	0.13	Long.	0.23	0.30	0.29
	10	28.0	28.00	12.00	2.88	3.60	0.40		0.46	0.57	0.56
	12	33.6	28.00	12.00	2.88	3.60	0.54		0.55	0.66	0.65
	15	42.0	28.00	12.00	2.88	3.60	0.79		0.69	0.79	0.78
	18	50.4	28.00	12.00	3.60	4.50	1.02		0.90	0.81	0.81
	20	56.0	28.00	12.00	4.80	6.00	1.16		1.13	0.77	0.76
	25	70.0	28.00	12.00	4.80	6.00	1.70		1.41	0.91	0.90
15	5	14.0	27.00	24.00	8.40	13.55	0.17	Torsion	0.20	0.19	0.18
	10	28.0	27.00	24.00	8.40	13.55	0.49		0.39	0.40	0.39
	12	33.6	27.00	24.00	8.40	13.55	0.65		0.47	0.47	0.47
	15	42.0	27.00	24.00	8.40	13.55	0.92		0.59	0.57	0.57
	18	50.4	27.00	24.00	10.50	16.94	1.16		0.78	0.60	0.59
	20	56.0	27.00	24.00	14.00	22.58	1.32		0.97	0.57	0.56
	25	70.0	27.00	24.00	14.00	22.58	1.84		1.21	0.68	0.67
16	5	14.0	32.00	26.00	9.40	15.00	0.17	Torsion	0.19	0.17	0.17
	10	28.0	32.00	26.00	9.40	15.00	0.49		0.39	0.36	0.36

Table 1 (continued)

Plan No.	No. of story	Height (m)	Dimension (m)		Shear-wall area (m <sup>2</sup> )		FEM results		Predicted period, $T$ (s)		
			Length	Width	Length	Width	$T$ (s)	First mode	Eq. (1)	TSC98	UBC97
	12	33.6	32.00	26.00	9.40	15.00	0.64		0.47	0.43	0.43
	15	42.0	32.00	26.00	9.40	15.00	0.88		0.58	0.53	0.52
	18	50.4	32.00	26.00	11.75	18.75	1.10		0.77	0.55	0.55
	20	56.0	32.00	26.00	15.67	25.00	1.24		0.96	0.52	0.51
	25	70.0	32.00	26.00	15.67	25.00	1.69		1.20	0.62	0.62
17	5	14.0	24.00	14.00	4.80	7.44	0.17	Torsion	0.25	0.28	0.28
	10	28.0	24.00	14.00	4.80	7.44	0.48		0.50	0.55	0.54
	12	33.6	24.00	14.00	4.80	7.44	0.63		0.60	0.64	0.63
	15	42.0	24.00	14.00	4.80	7.44	0.88		0.75	0.77	0.76
	18	50.4	24.00	14.00	6.00	9.30	1.12		0.99	0.79	0.79
	20	56.0	24.00	14.00	8.00	12.40	1.29		1.23	0.75	0.74
	25	70.0	24.00	14.00	8.00	12.40	1.80		1.54	0.89	0.88
18	5	14.0	16.00	12.00	3.84	8.16	0.11	Torsion	0.27	0.32	0.32
	10	28.0	16.00	12.00	3.84	8.16	0.26		0.54	0.60	0.60
	12	33.6	16.00	12.00	3.84	8.16	0.33		0.64	0.70	0.69
	15	42.0	16.00	12.00	3.84	8.16	0.45		0.80	0.82	0.83
	18	50.4	16.00	12.00	4.80	10.20	0.59		1.06	0.86	0.85
	20	56.0	16.00	12.00	6.40	13.60	0.68		1.32	0.81	0.80
	25	70.0	16.00	12.00	6.40	13.60	1.03		1.64	0.96	0.95
19	5	14.0	28.00	12.00	5.76	6.00	0.13	Torsion	0.29	0.30	0.29
	10	28.0	28.00	12.00	5.76	6.00	0.40		0.59	0.57	0.56
	12	33.6	28.00	12.00	5.76	6.00	0.54		0.70	0.66	0.65
	15	42.0	28.00	12.00	5.76	6.00	0.79		0.88	0.79	0.78
	18	50.4	28.00	12.00	7.20	7.50	1.02		1.15	0.81	0.81
	20	56.0	28.00	12.00	9.60	10.00	1.16		1.44	0.77	0.76
	25	70.0	28.00	12.00	9.60	10.00	1.70		1.79	0.91	0.90
20	5	14.0	16.00	12.00	3.84	5.76	0.12	Trans.	0.25	0.33	0.33
	10	28.0	16.00	12.00	3.84	5.76	0.31		0.50	0.61	0.62
	12	33.6	16.00	12.00	3.84	5.76	0.39		0.61	0.70	0.72
	15	42.0	16.00	12.00	3.84	5.76	0.52		0.76	0.82	0.87
	18	50.4	16.00	12.00	4.80	7.20	0.64		0.99	0.90	0.89
	20	56.0	16.00	12.00	6.40	9.60	0.73		1.24	0.85	0.84
	25	70.0	16.00	12.00	6.40	9.60	1.06		1.55	1.01	1.00

Long. implies longitudinal direction; Trans. implies transverse direction.

based on the finite element analyses of 20 different buildings (most have as-built plans and were already constructed). Each building was studied for seven different story levels (i.e., 5, 10, 12, 15, 18, 20 and 25). Shear-wall thickness was taken as 12 cm for buildings up to 15-story, 15 cm for 18-story buildings and 20 cm for 20- and 25-story buildings. The database compiled constitutes 140 buildings, their plan dimensions, number of stories and height, plan shear-wall areas in two directions as well as computed fundamental periods using 3D FEM analyses. This ensemble is presented in Table 1. The equation developed to predict the fundamental period of the tunnel form buildings has the following form:

$$T = Ch \frac{\sqrt{R}}{(R_{\text{length}}^a + R_{\text{width}}^a)} \quad (1)$$

where  $T$  is the period in s;  $h$  is the total height of building in m;  $R$  is the ratio of long side dimension to short side dimension of the building;  $R_{\text{length}}$  is the ratio of shear-wall area oriented along the length to a typical story area; and  $R_{\text{width}}$  is the ratio of shear-wall area oriented along the width to typical story area. In this equation,  $C$  and  $a$  are the estimator parameters obtained from regression analysis, and are equal to 0.138 and  $-0.4$ , respectively. The results obtained are also used to compute the associated errors in the estimation. The standard deviation of residuals,  $\sigma_T$ , expressing the random variability of periods, is 0.3 and the value of  $R^2$  (i.e., indication of goodness of fit) is equal to 0.80. There is no significant bias observed from the investigation of the residuals. Eq. (1) is similar to code equations (e.g., UBC and TSC) except for the three new parameters that we introduced. Analysis of results herein and from our earlier studies shows

that tunnel form buildings are significantly susceptible to torsion (see Table 1 for the first mode deformed shapes of the buildings) due to the plan shear-wall configuration that is restricted by the tunnel form construction technique. To account for this behavior and the effects of shear-walls into the period estimation, an additional parameter  $R$  is plugged into Eq. (1) incorporating two other new parameters,  $R_{width}$  and  $R_{length}$ .

### 3. Comparison with code-given period equations

Performance of Eq. (1) is next compared with code equations given in both the TSC and UBC. The TSC concerning constructions in seismic areas has been recently modified in 1998. In TSC, the equation for predicting the fundamental period of structures was taken directly from the UBC [23] with small modifications. The general form of the equation given in these provisions is as follows (note that the equations are in SI unit system):

$$T = C_t(h_n)^{3/4} \tag{2}$$

where  $T$  is the period in s;  $h_n$  is the height of the building in m;  $C_t = 0.0853$  (0.08) for steel moment-resisting frames,  $C_t = 0.0731$  (0.07) for reinforced concrete moment-resisting frames and eccentrically braced frames, and  $C_t = 0.0488$  (0.05) for all other buildings. Alternatively, the value of  $C_t$  for structures where seismic loads are fully resisted by reinforced concrete structural walls, can be taken as  $0.0743$  (0.075)/ $A_c^{1/2}$  ( $\leq 0.05$ ). The numbers within the parentheses show the corresponding values given in the TSC. The value of  $A_c$  can be calculated from the following

formula:

$$A_c = \sum A_e \left[ 0.2 + (D_e/h_n)^2 \right] \tag{3}$$

where  $A_e$  is the minimum cross-sectional area in any horizontal plane in the first story in  $m^2$  of a shear-wall;  $D_e$  is the length, in m, of a shear-wall in the first story in the direction parallel to the applied forces. The value of  $D_e/h_n$  used in Eq. 3 should not exceed 0.9. The period estimation via Eq. (1) and also the UBC and TSC equations are compared in Fig. 2 for various buildings in the database. Also shown in this figure are the finite element analysis results as benchmark solutions. Comparisons show significant deviation between the FEM results and those computed using code equations. For many cases, the code equations give a period much longer than those computed for low- and mid-rise (i.e., 5, 10 and 12 story) buildings, whereas for high-rise buildings (i.e., stories  $\geq 15$ ) the reverse is observed, and they underestimate the computed periods. In fact, the estimated periods should be the same or less than the actual period of the structure; hence, their estimation should be conservative. In general, comparisons reveal that there is a good correlation between the estimated periods via Eq. (1) and FEM results. For some of the 5-story buildings in the database, our equation could not capture the computed periods, and estimations result in higher deviation and become non-conservative.

### 4. Comparison with experimental data

The estimated periods using Eq. (1) are next compared with experimental data of Celebi et al. [14] and

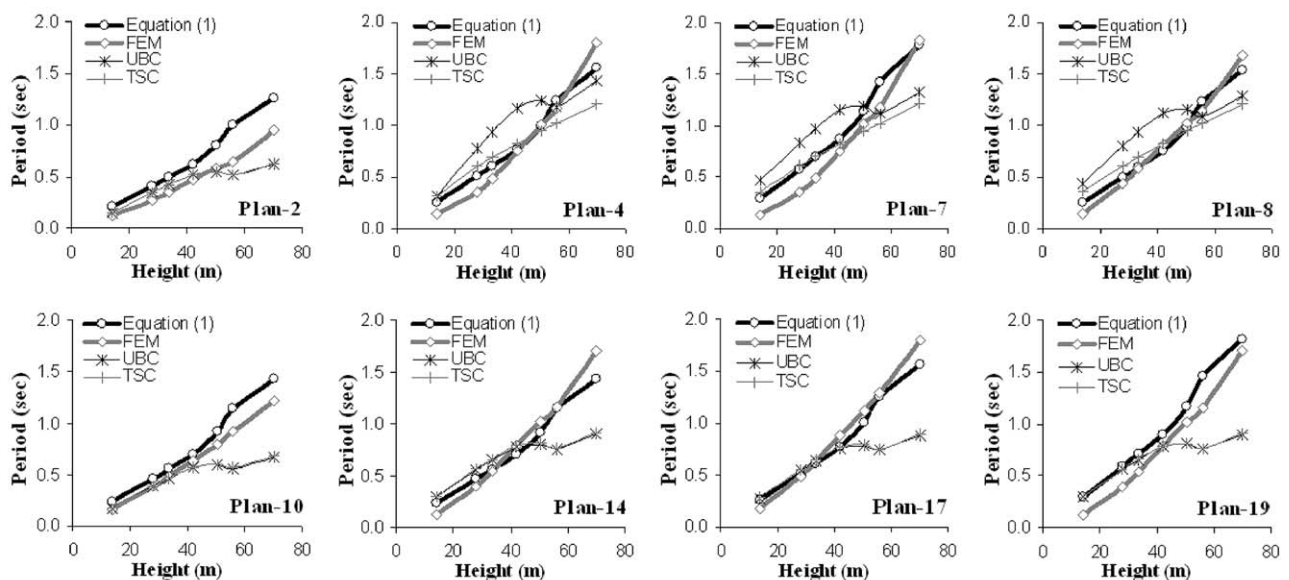


Fig. 2. Comparison of predicted periods via Eq. (1) with FEM, UBC (1997) and TSC (1998) expressions.

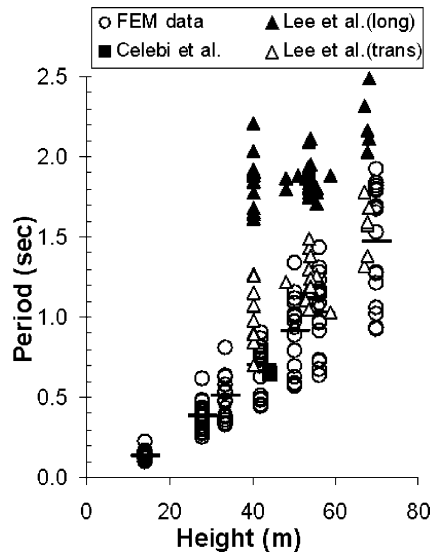


Fig. 3. Distribution of periods in Celebi et al. [14] and Lee et al. [25] and our database (Table 1), with respect to building height (solid bars denote mean of periods at a specific height for the buildings in Table 1; *long* stands for longitudinal direction; *trans* stands for transverse direction).

Lee et al. [25]. Celebi et al. measured the fundamental period of a mid-rise tunnel form building with and without outside panel configuration (note that outside panel wall is a nonstructural component). Most recently, Lee et al. conducted ambient surveys on 50 high-rise tunnel form buildings having 15–25 stories. Their building inventory has a wall thickness of 20 cm. Fig. 3 shows these compiled experimental data and the fundamental periods of the structures in our database. The details of the buildings where ambient surveys were conducted are given in Table 2 including their plan dimensions, heights and plan shear-wall areas. The estimated fundamental periods via Eq. (1) are also given in this table for comparison. The experimental data presented on the first 50 buildings have two periods, first along longitudinal direction and second along transverse direction. On the other hand, Eq. (1) is aimed at estimating the fundamental period regardless of the direction, attempting to consider the shear-wall configuration along both longitudinal and transverse directions as well as the effects of possible torsion. Therefore, it may only yield a single value assumed as the fundamental period. Based on this premise, the comparisons show that Eq. (1) gives estimates close to periods along the longitudinal direction for the majority of the buildings, but for only a few cases underestimates transverse periods or overestimates longitudinal periods. These results imply that Eq. (1) is generally conservative as expected from any code-given equations. In fact, the period of the structures elongates during inelastic response because of the stiffness degradation. Hence, Eq. (1) can be used to estimate the

lower bound fundamental period of tunnel form buildings having stories 5–25. In this study, the effects of nonstructural components (e.g., outside panel walls) as well as local-site effects on period estimation were ignored (i.e., fixed support conditions are assumed in all computer models); yet soil–structure interactions have been part of our ongoing research. It should also be noted that the proposed equation in this paper is based on the general consensus of engineering applications. Pending the accumulation of additional new data from the experimental studies and analyses of different buildings, the derived equation here can be progressively modified and improved.

## 5. Analytical model development for nonlinear analysis

In order to evaluate the 2D and 3D nonlinear seismic response of tunnel form buildings, 2- and 5-story buildings were selected as representative case studies. The plan and elevations of the buildings are shown in Fig. 4. Their structural systems are composed of solely shear-walls and slabs having the same thickness (12 cm) as in usual applications. Equal slab and wall thickness (12–20 cm) of tunnel form buildings, generally less than those of the conventional RC structures, results in significant slab–wall interaction, and tunnel form buildings behave like thin-wall-tubular structures where in-plane rigidity is low [12]. Thus, high stress-concentration may increase the crack propagation at the edges of the slab–wall connections. Therefore, a rigid diaphragm assumption (infinitely rigid in their own plane) to simplify the analysis and save from the run-time may not warrant realistic solutions. To account for in-plane floor flexibility, shear-walls and slabs were modeled using finite elements having both flexural and membrane capabilities (explained further in the forthcoming section). A nonlinear shell element was developed for that purpose using an isoparametric serendipity interpolation scheme with 5 d.o.f. at each node. This form of element description was selected in order to have a variable edge order and arbitrarily placed movable edge nodes (to consider the location and amount of discrete reinforcement bars near the edges and around the openings). This new element was implemented to a general purpose finite element program, POLO-FINITE [35]. The capability of moving any of the element edge nodes to any location along an edge allows these edge nodes to be placed in a proper position where they can serve as end nodes for the cover of a discrete reinforcement bar. This provides a robust stiffness contribution coming from the main reinforcement [9]. Besides arbitrarily movable edge nodes, the advantage of a variable edge order in the finite element modeling can be put to good use when

Table 2  
Experimental period data

Plan No. <sup>a</sup>	No. of story	Height (m)	Dimension (m)		Shear-wall area (m <sup>2</sup> )		Measured period, <i>T</i> (s)		Predicted period, <i>T</i> (s)
			Length	Width	Length	Width	Long. <sup>b</sup>	Trans. <sup>b</sup>	Eq. (1)
1	15	40.0	38.98	11.26	13.17	24.58	1.92	0.71	1.42
2	15	40.0	27.22	12.83	10.48	18.16	N/A <sup>b</sup>	1.08	1.10
3	20	53.5	30.94	12.38	9.96	17.62	1.89	1.19	1.51
4	20	53.5	31.66	12.02	10.66	15.98	1.90	1.44	1.55
5	20	53.5	30.94	10.88	9.43	18.18	1.93	N/A	1.68
6	15	40.0	49.22	11.61	8.00	22.86	N/A	1.27	1.24
7	15	40.0	27.22	12.83	8.38	18.16	2.22	N/A	1.04
8	15	40.0	56.28	12.47	18.25	35.09	1.86	1.16	1.54
9	15	40.0	28.14	12.47	9.12	18.95	1.66	1.09	1.10
10	15	40.0	34.46	12.47	11.17	22.35	1.93	N/A	1.21
11	20	53.5	42.20	12.14	13.32	24.59	2.11	N/A	1.79
12	15	40.0	38.98	11.28	13.19	21.98	1.63	N/A	1.39
13	15	40.0	27.22	12.83	8.38	19.56	2.05	0.91	1.06
14	20	53.5	41.80	11.18	14.95	21.50	1.82	1.16	1.93
15	20	53.5	37.20	12.36	14.71	19.31	1.95	N/A	1.70
16	20	53.5	45.40	11.94	17.35	22.77	1.88	N/A	1.92
17	20	53.5	45.40	11.94	18.43	22.77	1.82	1.50	1.94
18	20	53.5	32.00	11.94	12.99	16.81	1.76	N/A	1.64
19	15	40.0	51.90	10.36	16.13	31.19	1.91	0.90	1.72
20	15	40.0	34.60	10.36	10.75	21.51	N/A	0.86	1.41
21	15	40.0	61.80	11.80	21.88	36.46	1.89	1.28	1.71
22	15	40.0	41.60	11.80	13.74	25.53	N/A	0.99	1.39
23	15	40.0	53.40	10.80	14.99	32.30	N/A	1.16	1.64
24	15	40.0	36.60	11.90	13.07	23.52	1.92	1.27	1.33
25	15	40.0	35.60	10.80	13.07	22.30	1.79	N/A	1.43
26	15	40.0	42.90	11.00	16.04	22.65	1.65	N/A	1.51
27	18	48.1	43.40	11.62	11.09	24.21	1.81	N/A	1.61
28	20	53.5	34.64	10.73	11.89	20.81	1.85	1.17	1.86
29	18	48.1	34.60	12.50	12.98	19.90	1.88	1.23	1.47
30	20	53.0	53.60	11.40	17.11	23.22	1.88	1.12	2.01
31	20	53.5	29.44	11.40	9.40	13.42	1.83	N/A	1.52
32	20	53.5	35.48	11.40	12.13	16.18	1.91	1.31	1.69
33	20	53.5	52.50	10.92	18.35	32.10	1.79	1.06	2.27
34	22	58.9	52.50	10.92	18.35	33.25	1.89	1.04	2.52
35	25	67.0	43.40	12.12	12.62	24.20	2.33	1.79	2.22
36	25	67.0	35.00	10.92	11.47	22.93	N/A	1.33	2.32
37	25	67.9	38.10	12.30	11.25	22.49	2.56	1.39	2.11
38	25	67.9	20.80	11.50	7.65	13.40	2.04	1.59	1.77
39	25	67.9	27.30	12.00	7.21	16.38	2.17	1.61	1.79
40	25	68.0	63.90	11.50	14.70	33.80	2.50	N/A	2.69
41	25	68.0	51.84	12.60	16.98	27.43	2.13	1.69	2.42
42	19	51.1	36.80	11.20	13.19	23.08	1.89	N/A	1.79
43	20	53.9	36.80	11.20	13.19	21.43	1.79	1.25	1.87
44	15	40.0	18.30	10.70	4.31	11.75	1.69	0.90	0.94
45	20	55.6	35.60	11.40	15.42	13.80	1.79	N/A	1.79
46	20	55.6	53.40	11.40	19.48	20.70	1.72	1.25	2.12
47	20	55.6	41.60	12.00	13.98	24.96	1.82	1.27	1.91
48	20	54.0	31.80	10.00	8.27	17.81	N/A	1.25	1.78
49	20	54.0	51.20	11.60	13.07	26.13	1.96	1.39	1.93
50	20	54.0	50.40	12.30	11.16	33.48	2.13	1.20	1.84
51	15	44.1	20.86	19.08	9.56	15.32	0.66	N/A	0.78

<sup>a</sup> Experimental data from 1 to 50 comes from Lee et al. [25]; data of 51 comes from Celebi et al. [14].

<sup>b</sup> Long. implies longitudinal direction; Trans. implies transverse direction; N/A stands for not available.

the stress gradients are expected to be high. This allows increasing the order of displacement field in critical areas such as those around openings and slab–wall connections. The matching of the displacement fields

between different order finite elements can be adjusted to retain the compatibility along their common edges. Another improvement from the use of this new element is the reduction in the capacity and computational time

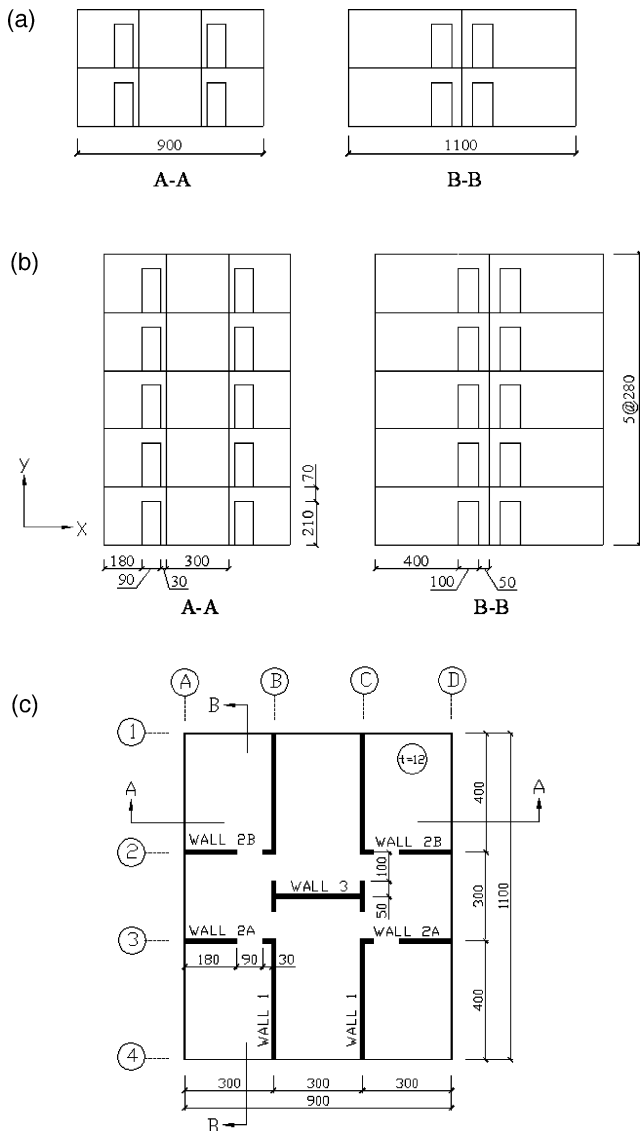


Fig. 4. Typical plan and elevations for 2- and 5-story buildings (units are in cm). (a) 2 story elevation; (b) 5 story elevation; (c) plan view.

required to reach a solution while retaining the level of accuracy deemed desirable. To reduce the computational time as well as the capacity associated with the 3D modeling of incorporating new shell element, a mixture of finite elements of different order was used. Higher order finite elements were utilized at the critical locations where stress concentrations or stress gradients were expected to be high.

In computer simulations, shear-walls were modeled as attached to fixed base supports. Any foundation and site effects were ignored. This may increase the computed overturning base moments. In this study, the shape of the stress–strain curve, tension stiffening and the cracking having opening and closing capability [18,26] were considered in the context of material non-

linearity, and the geometric nonlinearity was ignored due to the relatively small deformation obtained.

### 5.1. Reinforcement modeling

Finite element modeling of the reinforcement in a reinforced concrete member can be handled in a number of different ways. The steel can be considered as discrete steel elements, as individual steel units embedded in a concrete element, or as a smeared layer of steel sandwiched within the concrete layers. In the discrete steel model, reinforcing bars can be modeled using special rod elements located between prescribed element edge nodes. In general, these are two noded elements that present compatibility discontinuities with the adjacent concrete unit. Higher order elements can be used along the edges of comparable order concrete elements. If a higher order element is desired with the steel placed to pass through the interior of an element, an embedded steel element should be preferred. On the other hand, the smeared reinforcement model is the easiest to implement, and it can transfer the effects of the steel (i.e., strength and stiffness) directly into the concrete element. In this study, nonlinear rod elements having elasto-plastic stress–strain characteristics were used around the openings and near the edges (see Fig. 5). With the help of the developed isoparametric shell element, the discrete steel could be included while locating the rebars with proper concrete cover requirements. With a two noded rod element, the stiffness contributed only to its end nodes. For this case, the bond was neglected due to the incompatible nature of the two displacement fields defining the deformations of the steel and concrete. In this study, the smeared steel model was used as the general reinforcement for non-critical locations. It was treated as an equivalent uniaxial layer of the material at the appropriate depth and smeared out over the element as several orthotropic layers. The steel was taken into account in both faces of the slabs and shear-walls, and in both principal directions considering the minimum steel ratio and cover thickness.

The reinforcements were modeled as discrete or embedded based on the criticality of their locations. The minimum amount of steel percentage for shear-walls and slabs is 0.4% of the section area in accordance with the ACI 318-95 [2] specifications. There were also additional longitudinal and diagonal reinforcement used in the modeling in the form of two #4 (13 mm in diameter) at the inner and outer faces of the edges, and two #4 around the openings as shown in Fig. 5. The material properties of the concrete and the steel used in the analytical models are presented in Table 3.

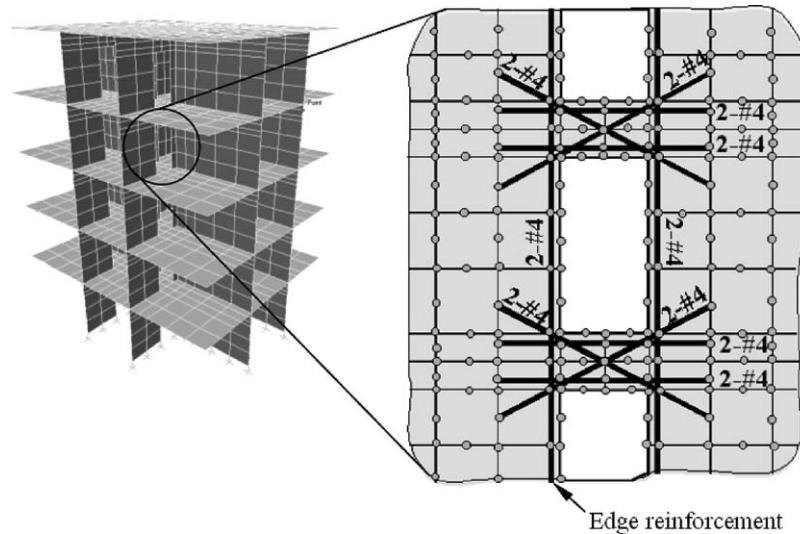


Fig. 5. 3D finite element modeling of 5-story building, and its edge and diagonal reinforcement detailing around openings.

### 5.2. Concrete crack modeling

Cracks in concrete can be modeled either as a smeared or a discrete crack model. In the smeared crack modeling, there are several options. They can be modeled either as a fixed-crack or as a rotational-crack. In most of the finite element analyses of RC structures, crack directions are assumed to be fixed; this means when the crack forms it remains open. However, this model leads to crack directions that can be inconsistent with the limit state [19]. The change in the crack direction and the resultant change in the direction of the maximum stiffness were clearly observed in the experiments of Vecchio and Collins [38]. Therefore, the need for an algorithm that accounts for this rotating crack effects is inevitable. In fact, the rotating crack models represent the actual behavior more accurately [26]. The constitutive matrix derived by Gallegos-Cezares and Schnobrich [18] was implemented for that purpose. The important concrete cracking behavior was handled through the smeared crack concept that has a rotation as well as closing and opening capabilities.

Table 3  
Material properties of concrete and steel

Concrete	Steel	Steel rod element
$E = 2.14 \times 10^6 \text{ t/m}^2$	$E = 2 \times 10^7 \text{ t/m}^2$	$E = 2 \times 10^7 \text{ t/m}^2$
$\nu = 0.2$	$\nu = 0.3$	$\nu = 0.3$
$f_{tu}/f_{cu} = 0.06823$	$Q_s(\text{top}) = 0.2\%$ in both directions	$A_s = 0.000226 \text{ m}^2$ (at openings)
$f_{c28} = 1925 \text{ t/m}^2$	$Q_s(\text{bottom}) = 0.2\%$ in both directions	$A_s = 0.000452 \text{ m}^2$ (at edges)
	$f_y = 22,000 \text{ t/m}^2$	$f_y = 22,000 \text{ t/m}^2$

### 5.3. Analytical model verification

Two types of studies were carried out to verify the accuracy of the developed models. For shear-wall behavior, the Toronto University panel test results of Vecchio and Collins [38] were used to compare the experimental results with the computer simulations. For the behavior of shear-walls having openings, the scaled 5-story building tested at the University of Michigan [3,4] was used for cross-check. The crack patterns of the shear-walls in the finite element models were further compared with those observed during the earthquakes. Conformity of the comparisons promoted the use of the numerical model for the shear-wall dominant systems. Details of the verification studies can be found in elsewhere [9,10].

## 6. Seismic performance evaluation

Seismic performance evaluation of tunnel form buildings was achieved via capacity spectrum method as outlined in ATC-40 [8]. Pushover analyses on 2- and 5-story buildings were conducted to compute their capacity curves. The buildings were loaded first with gravity loads, then pushed (along  $y$ -direction in Fig. 4) with the incrementally increased lateral load distribution until the specified level of roof drifts was reached. The inverted triangle invariant static load pattern computed based on the UBC was used for this purpose. The buildings were also modeled two dimensionally considering only the main shear-walls (section B-B in Fig. 4).

As mentioned before, torsion is an important behavior appearing in the dynamic mode of tunnel form

buildings. This phenomenon may appear due to the restrictions of the tunnel form construction technique. As such outside facade panels during construction should be open to take the formwork back (see Fig. 1). The procedure to account for the effects of the torsion in the development of the capacity curves is explained in ATC-40. In our study, the existence of torsion in the first mode of the two buildings required modifications in the capacity curves as well. The resultant modified capacity curves for 2- and 5-story buildings are presented in Fig. 6. Also shown in this figure are the capacity curves for 2D and 3D models. The 3D models yield higher capacity in both cases. The 2-story building is more rigid than the 5-story building and results in significantly more capacity. For the 5-story building, the yielding occurred at the location of the shear-wall bases and the connection joints around the openings. In the 2- and 5-story buildings, the overall system behavior was completely controlled by the symmetrically distributed shear-walls (see Fig. 4).

The capacity spectrum method (CSM) was next utilized to identify the performance level of the buildings according to ATC-40. The CSM is assumed to uniquely define the structural capacity irrespective of the earthquake ground motion. In order to reach a comparable conclusion about the expected demand of the structure under the design earthquake level, the capacity curve should be plotted on the same format with the specified demand spectrum. The demand curve is represented by earthquake response spectra, and a 5% damped response spectrum is used to represent the elastic demand. The capacity curves were converted into the acceleration displacement response spectrum (ADRS) format for comparison with demand curves.

This procedure requires making modification on the capacity curve by the first mode modal mass coefficient and the modal participation factor. The effective vibration periods of the 2- and 5-story buildings were 0.073 and 0.230 s, respectively. The 2- and 5-story buildings were pushed to roughly 1.71 and 2.10 cm of displacement at the roof level. The structural behavior type was selected as *Type A* for both cases according to ATC-40. During the conversion of capacity curve to ADRS format, the procedure that requires change of fundamental period, and therefore corresponding equivalent damping as prescribed in ATC-40 [8] were taken into account. The obtained values of the modal participation factors ( $PF_{RF}$ ) and the effective mass coefficients ( $\alpha_m$ ) were 1.30 and 0.89 for 2-story, and 1.38 and 0.76 for 5-story building. The seismic demand was determined on the zone of high seismicity and soft soil site condition (Z4) according to the TSC. The corresponding seismic demand and capacity spectra are also plotted in ADRS format for comparison in Figs. 7a and 8a for 2- and 5-story buildings, respectively. The 2-story building possesses an energy dissipation capacity at the ultimate stage equivalent to 28.9% equivalent viscous damping for which the reduced demand spectrum intersect with its capacity spectrum at the small spectral displacement. The energy dissipation capacity of the 5-story building is less than that of the 2-story building and equal to 24.6% equivalent viscous damping. These results verify that the buildings are capable of satisfying the code requirements at the acceleration sensitive region of the design spectra. The capacity and demand intersect at a performance point where the roof displacement to the total height ratio is 0.003 and 0.0015 for 2- and 5-story

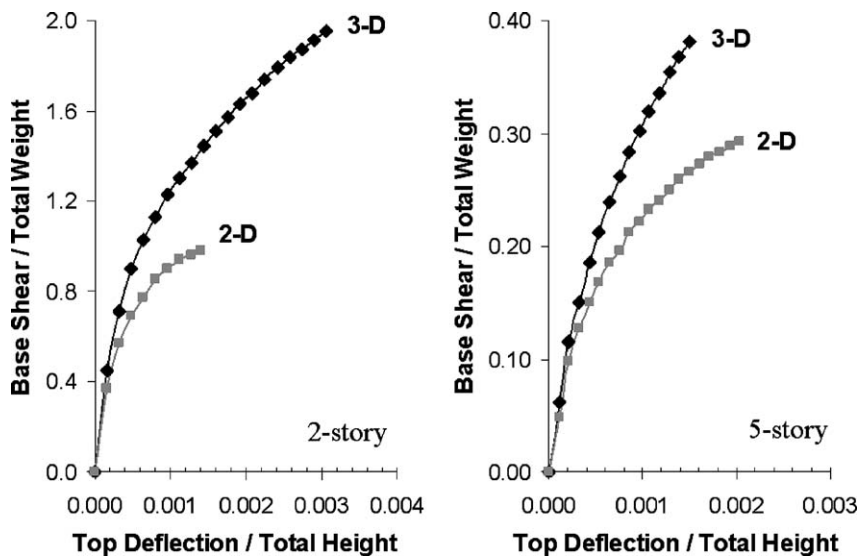


Fig. 6. Modified capacity curves for 2D and 3D models of 2- and 5-story buildings.

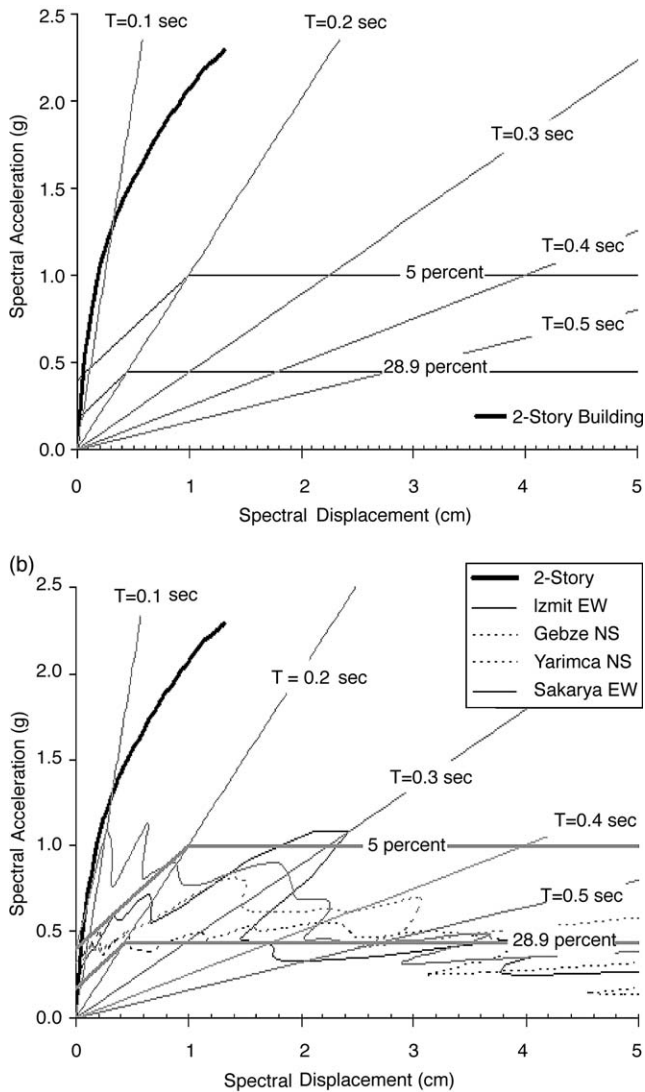


Fig. 7. Demand and capacity comparison for 2-story building using (a) TSC (1998) design spectrum (soft soil site condition); (b) 1999 Kocaeli earthquake ground motion records (5% damped).

buildings, respectively. At this level, the buildings are considered to satisfy the immediate occupancy (IO) performance level defined in the ATC-40. The performance point is 1.42 cm ( $S_d$ ) for the 5-story building as shown in Fig. 7a. This spectral displacement can be back translated to a roof displacement of 1.95 cm ( $\Delta_R = S_d \times PF\Phi_R$ ) and a base shear coefficient of 0.37 ( $V/W = \alpha S_a$ ).

In Figs. 7b and 8b, 5% damped response spectra of the NS and EW components of the 1999 ( $M_w$  7.4) Kocaeli (Turkey) earthquake ground motions are compared to capacity curves (Izmit EW 0.23 g PGA at 4.3 km from fault; Gebze NS 0.27 g PGA at 15 km; Yarimca NS 0.23 g PGA at 3.3 km; Sakarya EW 0.41 g PGA at 3.2 km). The comparison of the demand and response curves shows that the 2-story building eas-

ily reached the elastic demand spectra of the Kocaeli earthquake ground motions since it shows a significantly rigid behavior. The 5-story building capacity barely intersects with the elastic design spectrum.

### 7. 3D behavior and tension–compression (T/C) coupling

Tension–compression (T/C) coupling, executed by in-plane and membrane forces within the shear-walls, is a 3D originated mechanism forming in the tunnel form buildings due to wall-to-wall (including walls with openings) and wall-to-slab interactions. In this mechanism, the outer walls, oriented perpendicular to the lateral loading direction, act as a flange when subjected to bending loads, and resist the overall moment primarily in tension and compression. On the other hand, the inner walls, passing from the centroid and oriented to the same direction with the lateral loading, act in bending, and their contribution to overall moment capacity is smaller. In general, this 3D originated mechanisms show a characteristic T-section behavior. Therefore, the resultant force mechanism exhibits a significant contribution to the capacity and seismic performance. The development of T/C coupling mechanism in tunnel form buildings is illustrated in Fig. 9.

The analyses showed that part of the walls above the openings were deflected more in 2D models than in 3D models (Fig. 10). In 2D simulations, the T/C coupling was weakly accomplished with the transverse shear through the coupling beams, whereas the transverse walls in 3D cases stiffened the sections by providing additional paths for the shear transfer (Fig. 12). The local moment contribution coming from the main shear-walls was not altered significantly from 2D to 3D cases. This may be attributed to the limitation in contribution of steel (i.e., limited to steel area and its yield stress). When the analysis was switched from 2D to 3D, transverse walls provided an extra resistance. This resulted in substantial increase in the lateral load carrying capacity. The deflected shape of the 2-story building showed that the behavior of the structure was dominated by in-plane and membrane forces. The overturning base moments and resultant coupling forces were computed considering contribution of couple walls to observe significance of 3D behavior. The total overturning moment capacity of the 2-story building at its failure load level was found to be 2130 kN m (213 ton m) in the 2D model. When the 3D model was considered at this load level, the moment capacity reached 1703 kN m (170.3 ton m) and gradually increased up to 4420 kN m (442 ton m) at its failure load level. This step up was accredited to the increase in the tension and compression forces that were present

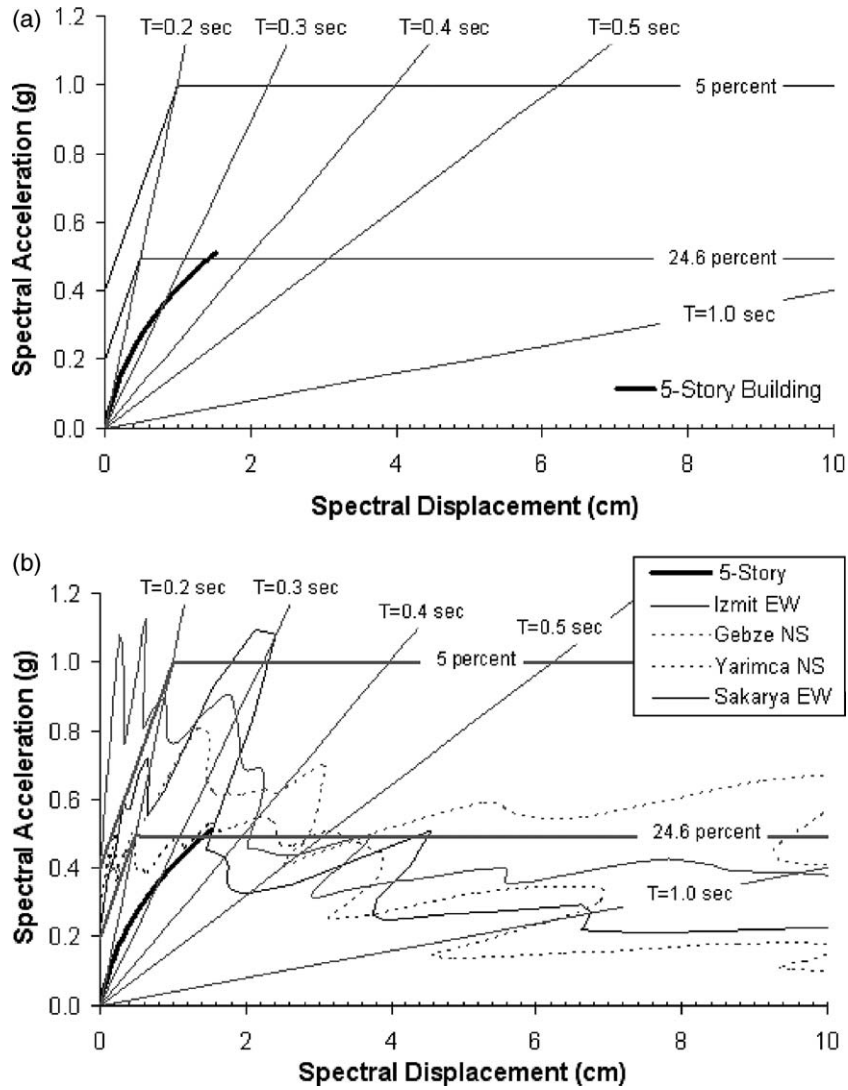


Fig. 8. Demand and capacity comparison for 5-story building using (a) TSC (1998) design spectrum (soft soil site condition); (b) 1999 Kocaeli earthquake ground motion records (5% damped).

in the longitudinal walls and their coupling effects with the transverse walls. A similar behavior was observed for the 5-story building as well.

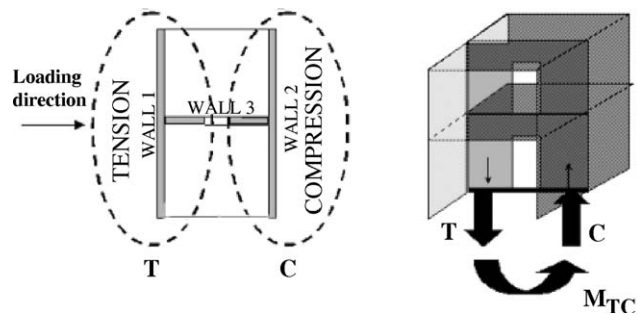


Fig. 9. Slap-wall interaction due to tension and compression (T/C) coupling mechanism.

### 8. Influence of flexible diaphragms on dynamic behavior

The influence of flexible diaphragms on the dynamic behavior of structures gains more significance particularly for thin-wall structures. Although the conceptual details were given in Tena-Colunga and Abrams [36], and Fleischman and Farrow [16], for the integrity of the concept the contribution of out-of-plane bending on tunnel form building behavior is illustrated in a simple 3D model described in Fig. 11a. This 2-story building was laterally loaded in a similar fashion as explained previously for 2- and 5-story buildings. The moment distributions at the base of the shear-walls were separated into their components coming from the main wall (Wall-3), transverse walls (Wall-1 and -2) and the slab. The resultant free body diagram for Wall-

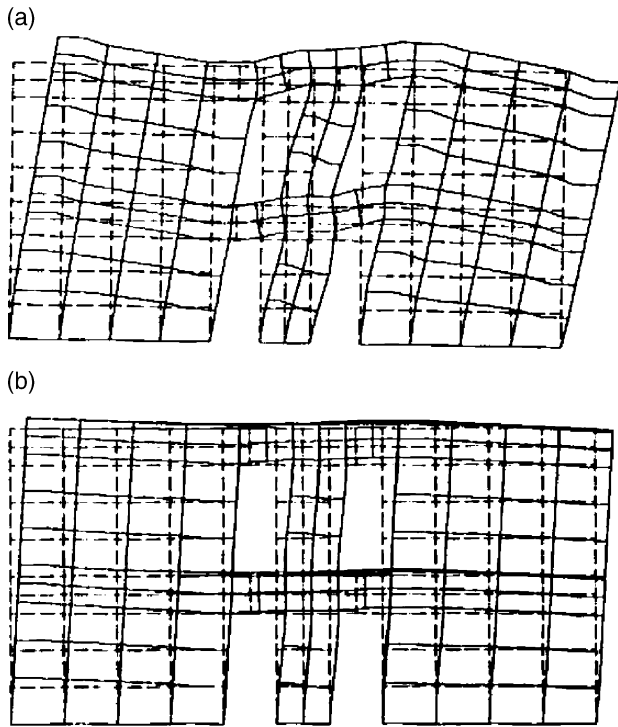


Fig. 10. Two-story building deflected shapes at failure load level. (a) 2D model; (b) 3D model.

3 (that contains an opening) is presented in Fig. 11b. In this figure,  $M_b$  denotes the slab bending moment. The moments acting on Wall-3 from Wall-1 and Wall-2 are in fact in-plane moments for Wall-3; however, they are out-of-plane moments for Wall-1 and Wall-2. Here, the transverse walls contribute to total acting moment on

Wall-3 with their out-of-plane moment components. That phenomenon strongly arises during the 3D behavior. Base moment from membrane forces due to tension/compression (T/C) couple is still dominant compared to out-of-plane moment component of transverse walls; yet, their contribution may increase when the opening size is large enough to decrease the T/C coupling moment [13].

### 9. Shear-wall openings and reinforcement detailing

In the tunnel form technique, the slabs are supported only along their three sides by shear-walls while one side remained unsupported in order to take the formwork back (Fig. 1). In common practice, these three shear-walls contain at least one opening for the functional use and access. The analyses show that the openings cause a strong disruption of the shear flow between the adjacent shear-walls. This phenomenon can be observed from the shear stress distribution of 2D and 3D models of the 5-story building in Fig. 12 (at the last loading step of pushover). Despite the door openings introducing a strong disruption of the shear flow, the effects of T/C coupling mechanism developed in the system are significant. In the 3D model of the 2-story building, vertical load resistance capacity at the corner of the openings is 80% more than its 2D counterpart. The effects of openings on the strength and deformation capacity of the shear-wall systems are generally different than those observed in conventional frame-wall systems due to the coupling effects of beams connecting the adjacent shear-walls. These differences

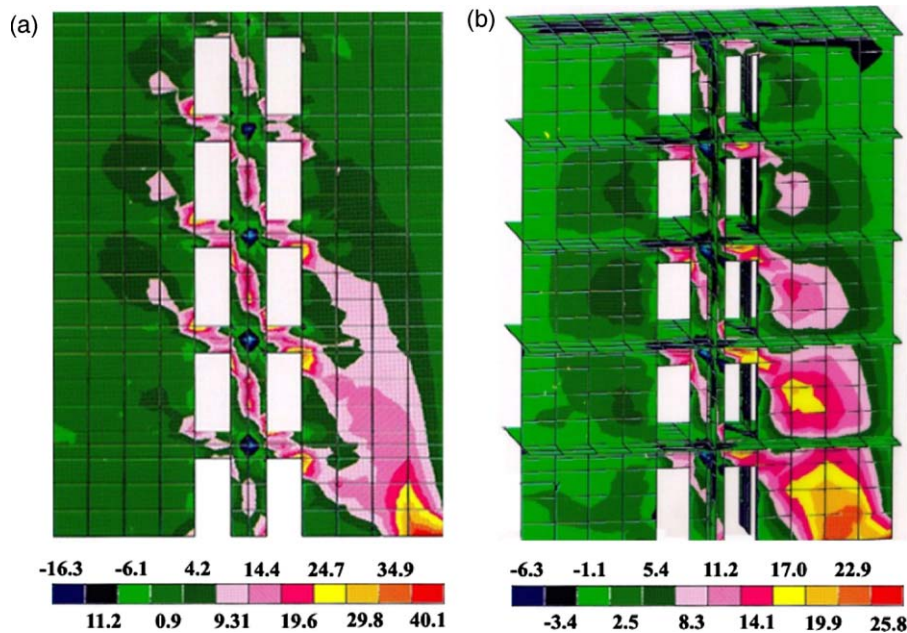


Fig. 12. Five-story building shear stress distribution (units are in m and ton).

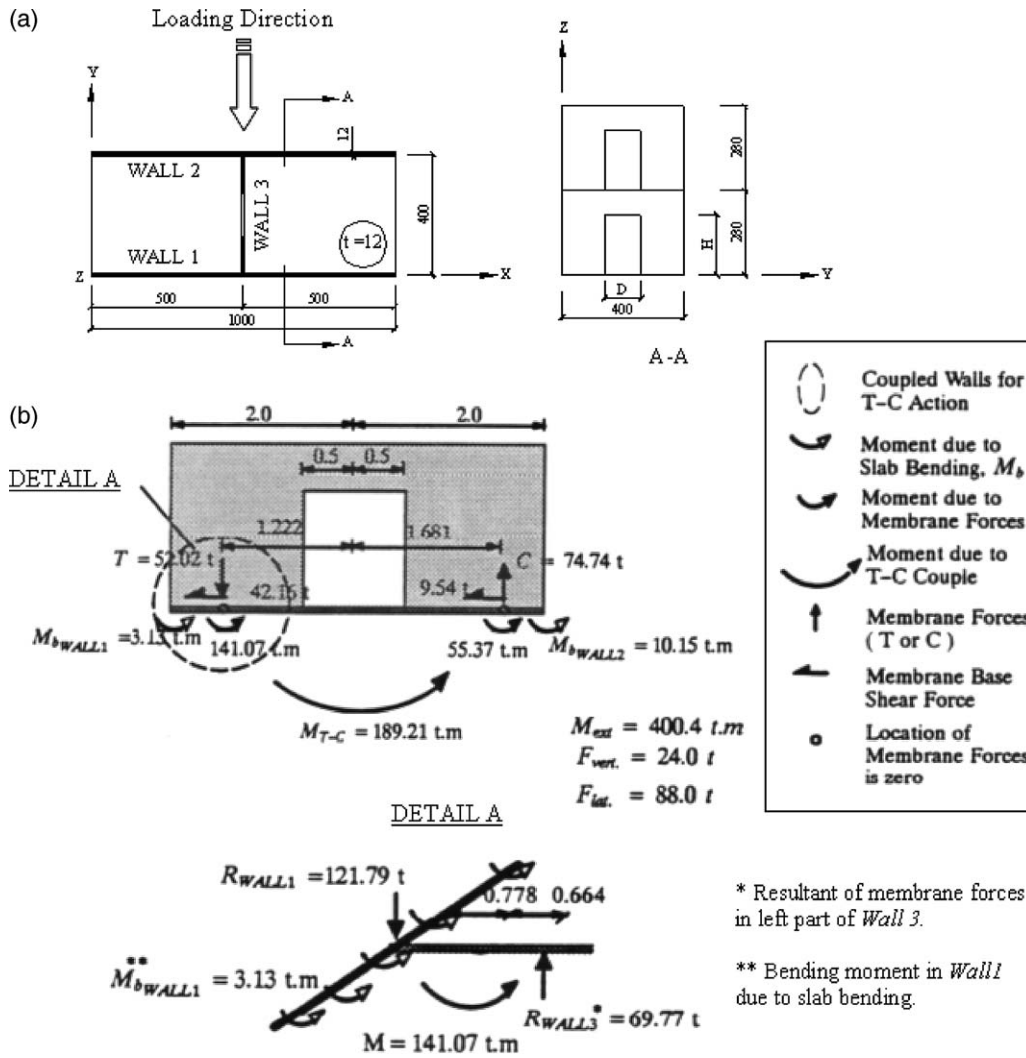


Fig. 11. (a) Plan and elevation view of a simple 3D model (physical dimensions are in cm); (b) Free body diagram of forces acting on Wall 3 (units are in m and ton).

are more evident when the 3D behavior is considered. In general, no contra-flexure points form above the openings as they do in the 2D coupled wall cases due to the restraint of motion by the existing transverse walls and slabs having a continuous edge support in the 3D.

Due to the nature of stress concentration around the openings, the use of the diagonal shear reinforcement in addition to edge reinforcement (i.e., longitudinal bars at both sides of openings as in Fig. 5) leads to a significant contribution for retarding and slowing down the crack propagation. In spite of this fact, current codes and seismic provisions present insufficient guidelines for the reinforcement detailing around the openings of pierced shear-walls particularly for the cases where there is no connection beam between two adjacent shear-walls. The ACI 318-95 [2] building code does not present any special reinforcement detailing as was found necessary around the openings. In the com-

mentary of this code, the shear strength calculation is given as it depends on the effective cross-sectional area of a wall considering the existing opening. A reasonable estimate for the lower bound of the shear strength of low-rise walls with minimum web reinforcement was presented by Wood in 1990 [40]. Additionally, the ACI 349 Nuclear Safety Structure Code [1] and the UBC [23] indicate that in addition to the minimum reinforcement in the walls, not less than two #5 (16 mm in diameter) bars shall be provided around the openings. The placement of diagonal shear reinforcement with an angle of  $45^\circ$  at the sections above the openings is recommended in the TSC. Due to the formation of high stress concentration around the openings, the use of the shear reinforcement as stirrups in the pierced part in addition to the edge reinforcement provides a significant confinement to the concrete covering the main longitudinal bars, and prevents the buckling of the bars and the premature shear failure. If diagonal

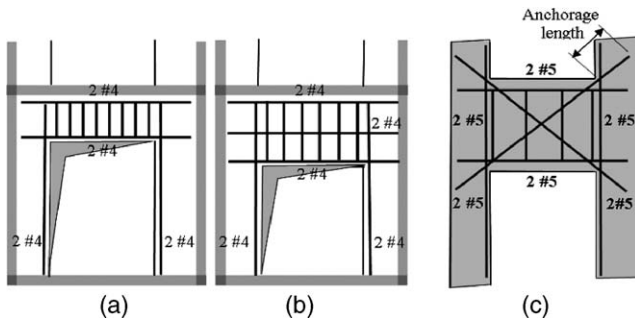


Fig. 13. Reinforcement detailing around the openings of pierced shear-walls.

bars are not provided, additional shear reinforcement can be used to resist the diagonal tension. The minimum amount of reinforcement and its detailing shown in Fig. 13a can be recommended for the pierced shear-walls in the case of existence of shallow sections above the openings (using two #4 as top and bottom bars, and two #4 at each vertical edge). Paulay and Binney [33] suggested the use of the diagonal reinforcement in deep coupling beams because of the relatively large shears that develop and the likelihood of shear failures under reversed cyclic loadings. Since the deep connections between shear-walls in the tunnel form buildings behave in a similar fashion, the reinforcement details given in Figs. 13b and c can be suggested when the wall part above the openings of the pierced walls is deeper. It should be also noted that the connecting beams should not be stronger than its adjacent piers that may cause earlier yielding of the piers before the deep beams would become inelastic. This further facilitates restricted ductility and poor energy dissipation under seismic excitation, and consequently soft story mechanism may result [34]. Therefore, the degrees of coupling between the wall parts considering the stiffness of the adjacent slabs and transverse walls in the three dimensions should be the basis for the reliable reinforcement detailing around the openings of the tunnel form buildings. It should be noted that the presented reinforcement detailing herein is based on the limited case studies investigated; numerous configurations of openings and reinforcement detailing should be evaluated for their generalization.

**10. Response modification factor**

In many seismic design codes and guidelines, such as UBC, NEHRP provisions [5] and TSC, reduction in seismic forces via response modification factor (*R*-factor) is justified by the unquantified overstrength and ductile response of buildings during design earthquake. However, none of these references addresses *R*-factor for RC buildings composed of solely shear-walls. For

that reason, it is aimed here to clarify the above using the results of previously discussed inelastic static push-over analysis of the 5-story building.

The values assigned to *R*-factor are generally intended to account for the period-dependent ductility factor ( $R_\mu$ ), period-dependent overstrength factor ( $R_S$ ), and redundancy ( $R_R$ ) factor. In this way, the *R*-factor can simply be expressed as their product [6]:

$$R = R_S \cdot R_\mu \cdot R_R \tag{4}$$

Recent developments in the displacement based design methodology [8,17] enable more quantitative evaluation of these factors. The relations exhibited in Fig. 14 can be established for that purpose. In this figure, the redundancy factor was developed as part of the project ATC-34 [7]. This is proposed to quantify the improved reliability of seismic framing systems that use multiple lines of vertical seismic framing in each principal direction of a building [39]. For our studied case, this factor equals to 1. For the evaluation of the other two factors, seismic design parameters, such as seismic zone, site geology, and fundamental period, must be clearly identified as a priori. Accordingly, the worst scenario (highest seismicity and soft-soil site condition) based on the TSC was chosen. This corresponds to a design base shear value of 0.25 *W* for the 5-story building. The overstrength factor ( $R_S$ ), which can be determined as the ratio of the maximum lateral strength of a building ( $V_u$ ) to the yield strength ( $V_{fy}$ ), envelops the global effects of story drift limitations, multiple load combinations, strain hardening, participation of nonstructural elements, and other parameters [37]. This relation and its sources have been the subject of much research in recent years [20,29,32]. To quantify this value, Hwang and Shinozuka [21] studied a four-story RC intermediate moment frame building located in seismic zone 2 as per the UBC [22], and they reported an overstrength factor of 2.2. Mwafy and Elnashai [30] performed both inelastic static pushover and time-history collapse analyses on 12 RC frame type build-

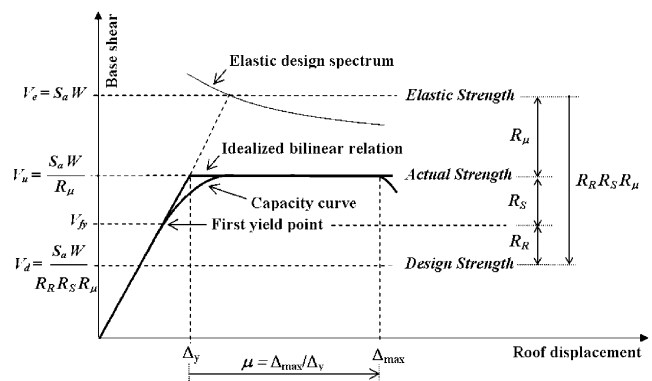


Fig. 14. Relationships between the response modification (*R*), ductility ( $R_\mu$ ), redundancy ( $R_R$ ) and overstrength ( $R_S$ ) factors.

ings designed based on the EC8 [15] codes and having various heights and lateral load supporting systems. They have declared that all studied buildings have overstrength factors over 2. For the investigated case here, the overstrength factor was calculated as 1.96. It is expected that their actual values may be higher than those estimated due to the contribution of non-structural components.

The ductility factor ( $R_{\mu}$ ) is a measure of the global nonlinear response of the system, and its quantification was reflected in many publications (e.g., [24,28,31]). Basically, this parameter can be expressed as the ratio of elastic to inelastic strength (e.g., [30]) as illustrated in Fig. 14. The resultant ductility factor was found as 2.0 for the 5-story building. It may yield to a response modification factor of 4.0 according to Eq. (4). The imposed  $R$ -factor in current seismic codes for RC frame type structures having shear-wall system that might be accepted as the closest form to tunnel form buildings is equal to 5.5 in the UBC [23] and 4.0 or 6.0 (depending on the ductility level) in the TSC. This comparison shows that values given in these references are admissible for the 5-story building investigated. It is certain that standardization of a response modification factor entails further investigations on numerous tunnel form buildings having different plan and height combinations.

## 11. Conclusions and recommendations

This paper reflects the breadth of the multi-scope study conducted on tunnel form buildings to identify their most essential seismic design parameters, and reveals the strong and weak points of the tunnel form system. Based on the investigations, the following conclusions can be delineated.

In general, performing linear or nonlinear detailed 3D finite element analyses on tunnel form buildings is difficult due to the existence of dominant shear-wall configurations, and most of time not conducted for design purposes. Therefore, code-given empirical formulas are commonly used to estimate the lower-bound fundamental period. Evidences based on the studies show that code-equations may lead to intolerable errors in estimating the periods of tunnel form buildings and consequently anticipated design loads for their reliable seismic design. An alternative formula is proposed in this paper to estimate the fundamental period of tunnel form buildings having stories 5–25. Comparisons with experimental studies show a good correlation and lend further credibility to its use in practice.

The performance evaluation of tunnel form buildings was accomplished by utilizing CSM on two representative cases to estimate their inelastic deformation demands. A widely used and popular approach to

establish these demand values is a ‘pushover’ analysis in which a model of the building structure is subjected to an invariant distribution of lateral forces. While such an approach takes into account for redistribution of forces following yielding of sections, it does not incorporate the effects of varying dynamic characteristics during the inelastic response. This is a major drawback of the invariant load patterns in pushover analysis. However, it was widely declared that such a load distribution may be adequate for regular and low-rise structures whose response is primarily in their fundamental mode. We believe that based on the small lateral deformation obtained and low-rise condition of the buildings that we investigated, use of an inverted triangle invariant load pattern could capture the response sufficiently.

Evaluation of response modification factor for the 5-story building yields a value of 4. In fact, actual response modification factor should be higher due to the remedial effects of nonstructural components. Clearly, numerous configurations of tunnel form buildings should be evaluated for its validity.

Notwithstanding the preferable seismic resistance of tunnel form buildings, limitations and restrictions of tunnel form system may result in torsion in the fundamental vibration mode. Selection of appropriate side dimensions and symmetrical configuration of shear-walls may help to eliminate or minimize the torsion. Although rectangular plans seem to be more preferable for avoiding torsion than square plans, buildings having rectangular plans may have weaker bending capacity along their transverse direction.

The results of this study showed that studies conducted on shear-wall dominant buildings without paying attention to the 3D effects of existing transverse walls may yield inaccurate and misleading results. In this study, the stress flow and crack patterns around the openings of pierced shear-walls in the 3D models are observed to be significantly different than those observed in the 2D models. The deflected shapes obtained for the sections above the openings in the 3D models exhibit more rigid forms than those in the 2D models. In general, considering the interaction effects of the slabs and transverse walls during the analyses increased the overall capacity of the pierced shear-walls. Despite the existence of openings introducing a strong disturbance of the shear flow within the transverse walls, these walls provided a significant contribution to the formation of T/C coupling mechanism.

The membrane action was found to be a dominant force mechanism for the tunnel form buildings, and the use of a nonlinear isoparametric shell element rather than a plane stress element in the finite element simulations provided a better representation of this mechanism. Additionally, use of this element enabled various modeling of the reinforcement in the models

based on the criticality of their locations. To investigate the local effects around the openings, simulation of reinforcement with discrete elements at such weak locations provided a detailed modeling of concrete cover for the development of more realistic crack patterns.

Due to the nature of high stress concentrations around the openings, the use of the diagonal shear reinforcement in addition to the edge reinforcement in these locations may lead to significant contribution for retarding and slowing down the crack propagation. For this reason, reinforcement details given in this study are recommended for various shear-wall opening configurations; yet, alternative reinforcement detailing should be evaluated to establish a conjectural basis.

Tunnel form buildings provide better seismic performance in addition to their low construction cost compared to conventional RC buildings. This in turn makes them an alternative building type to more costly base-isolated buildings in seismically active regions (e.g., California). For this reason, the intent of this study is to bring forward the good performance of these structures, and to identify their most important design parameters for practical applications.

## References

- [1] ACI 349. Commentary on code requirements for nuclear safety related concrete structures. ACI Manual Part 4, Nuclear Safety Structures Code. 1990. p. 349–360 [Chapter 14.3.4].
- [2] ACI 318. Building code requirements for reinforced concrete and commentary. ACI, Detroit, MI, 1995;73–4, 218, 242.
- [3] Aeja A, Wight JK. Reinforced concrete structural walls with staggered opening configurations under reversed cyclic loading. Department of Civil Engineering, University of Michigan, Report No: 90-05; 1990.
- [4] Aeja A, Wight JK. RC structural walls with staggered door openings. *J Struct Eng, ASCE* 1991;117(5):1514–33.
- [5] American Society of Civil Engineers (ASCE). Prestandard and commentary for the seismic rehabilitation of buildings, FEMA-356, Washington, DC; 2000.
- [6] ATC-19. Structural response modification factors. Redwood (CA): Applied Technology Council; 1995.
- [7] ATC-34. A critical review of current approaches to earthquake resistant design. Redwood (CA): Applied Technology Council; 1995.
- [8] ATC-40. Seismic evaluation and retrofit of concrete buildings. Redwood (CA): Applied Technology Council; 1996.
- [9] Balkaya C, Schnobrich WC. Nonlinear 3D behavior of shear-wall dominant RC building structures. *Struct Eng Mech* 1993;1(1):1–16.
- [10] Balkaya C. Nonlinear 3D behavior of shear wall dominant RC building structures. Ph.D. Dissertation, University of Illinois Urbana Champaign; 1993.
- [11] Balkaya C, Kalkan E. Estimation of fundamental periods of shear wall dominant building structures. *Earthquake Eng Struct Dyn* 2003a;32(7):985–98.
- [12] Balkaya C, Kalkan E. Nonlinear seismic response evaluation of tunnel form building structures. *Comput Struct* 2003b;81:153–65.
- [13] Balkaya C, Kalkan E. Three-dimensional effects on openings of laterally loaded pierced shear-walls. *J Struct Eng, ASCE* 2004;130(10).
- [14] Celebi M, Erdik M, Yuzugullu O. Vibration of multi-story RC structure cast in by tunnel forms. METU-EERI Report No: 77-6, Middle East Technical University, Ankara; 1977.
- [15] Comite European de Normalisation (CEN). Design provisions for earthquake resistance of structures. Part 1-1, 1-2 and 1-3. Eurocode 8, European pre-standard ENV 1998-1-1, 1-2 and 1-3. CEN, Bruxelles; 1994.
- [16] Fleischman RB, Farrow KT. Dynamic behavior of perimeter lateral system structures with flexible diaphragms. *Earthquake Eng and Struct Dyn* 2001;30:745–63.
- [17] FEMA-356. Prestandard and commentary for the seismic rehabilitation of buildings. Reston (VA): American Society of Civil Engineers (ASCE); 2000.
- [18] Gallegos-Cezares S, Schnobrich WC. Effects of creep and shrinkage on the behavior of reinforced concrete gable roof hyperbolic-paraboloids. *Struct Res Series* 1988;543 UIUC.
- [19] Gupta AK, Akbar H. Cracking in reinforced concrete analysis. *J Struct Eng, ASCE* 1984;110(8):1735–46.
- [20] Humar JL, Ragozar MA. Concept of overstrength in seismic design. Proceedings of the 11th WCEE. IAEE, Acapulco, Mexico, Paper No. 639; 1996.
- [21] Hwang H, Shinozuka M. Effect of large earthquakes on the design of buildings in eastern United States. Proceedings of the 5th US National Conference on Earthquake Engineering. Oakland (CA): Earthquake Engineering Research Institute; 1994. p. 223–231.
- [22] International Conference of Building Officials (ICBO). Uniform Building Code, Whittier, CA; 1994.
- [23] International Conference of Building Officials (ICBO). Uniform Building Code, Whittier, CA; 1997.
- [24] Kranwinkler H, Nassar AA. Seismic design based on ductility and cumulative damage demands and capacities. In: Fajfar P, Krawinkler H, editors. Nonlinear seismic analysis and design of reinforced concrete buildings. New York: Elsevier Applied Science; 1992.
- [25] Lee L, Chang K, Chun Y. Experimental formula for the fundamental period of RC buildings with shear-wall dominant systems. *Struct Design Tall Build* 2000;9(4):295–307.
- [26] Milford RV, Schnobrich WC. The application of the rotating crack model to the analysis of reinforced concrete shells. *Comput Struct* 1985;20:225–34.
- [27] Ministry of Public Works and Settlement. Turkish Seismic Code, “Specifications for structures to be built in disaster areas”, Ankara, Turkey; 1998.
- [28] Miranda E, Bertero VV. Evaluation of strength reduction factors for earthquake-resistant design. *Earthquake Spectra* 1994;10(2):357–79.
- [29] Mitchell D, Paulter P. Ductility and overstrength in seismic design of reinforced concrete structure. *Can J Civil Eng* 1994;21:1049–60.
- [30] Mwafy AM, Elnashai AS. Overstrength and force reduction factors of multistory reinforced-concrete buildings. *Struct Design Tall Build* 2002;11:329–51.
- [31] Newmark NM, Hall WJ. Earthquake spectra and design. Oakland (CA): Earthquake Engineering Research Institute; 1982.
- [32] Park R. Explicit incorporation of element and structure overstrength in the design process. Proceedings of the 11th WCEE. IAEE, Acapulco, Mexico, Paper No. 2130; 1996.
- [33] Paulay T, Binney JR. Diagonally reinforced coupling beams of shear-walls. *Shear in Reinforced Concrete* 1974;2(26):579–98 [ACI Special Publication, SP-42].
- [34] Paulay T, Priestley MJN. Seismic design of reinforced concrete and masonry buildings. New York: John Wiley & Sons, Inc; 1995. p. 744.
- [35] POLO-FINITE, Structural mechanics system for linear and nonlinear, static and dynamic analysis. Department of Civil Engineering, UIUC, 2003.

- [36] Tena-Colunga A, Abrams DP. Seismic behavior of structures with flexible diaphragms. *J Struct Eng, ASCE* 1996;122:439–45.
- [37] Uang C-M. Establishing  $R$  (or  $R_w$ ) and  $C_d$  factors for building seismic provisions. *Earthquake Eng Struct Dyn* 1994;23:507–21.
- [38] Vecchio FJ, Collins MP. The modified compression-field theory for reinforced concrete elements subjected to shear. *ACI Struct J Proc* 1986;83(2):219–31.
- [39] Whittaker A, Hart G, Rojahn C. Seismic response modification factors. *J Struct Eng, ASCE* 1999;125(4):438–44.
- [40] Wood SL. Shear strength of low-rise reinforced concrete walls. *ACI Struct J* 1990;87(1):99–107.